On long-range plasmonic modes in metallic gaps

David F. P. Pile[*], Dmitri K. Gramotnev[+], Rupert F. Oulton[*], Xiang Zhang[*]

[*]*NSF Nano-scale Science and Engineering Center, University of California, 5130 Etcheverry Hall, Berkeley, California 94720-1740*
d.pile@berkeley.edu, r.oulton@berkeley.edu, xiang@berkeley.edu

[+]*Applied Optics Program, School of Physical and Chemical Sciences, Queensland University of Technology, GPO Box 2434, Brisbane, QLD 4001, Australia*
d.gramotnev@qut.edu.au

Abstract: Satuby and Orenstein [Opt. Express **15**, 4247-4252 (2007)] reported the discovery and numerical and experimental investigation of long-range surface plasmon-polariton eigenmodes guided by wide (6 to 12 μm) rectangular gaps in 400 nm thick gold films using excitation of vacuum wavelength λ_{vac} = 1.55 μm. In this paper, we carry out a detailed numerical analysis of the two different types of plasmonic modes in these structures. We show that no long-range eigenmodes exists for these gap plasmon waveguides, and that the reported "modes" are likely to be beams of bulk waves and surface plasmons, rather than guided modes of the considered structures.

OCIS codes: (240.6680) Surface Plasmons; (230.7380) Waveguides, channeled.

References and links

1. D. F. P. Pile, T. Ogawa, Y. Matsuzaki, K. C. Vernon, K. Yamaguchi, T. Okamoto, M. Haraguchi, M. Fukui, "Two-dimensionally localized modes of a nanoscale gap plasmon waveguide," Appl. Phys. Lett. **87**, 261114 (2005).
2. G. Veronis, S. Fan, "Guided subwavelength plasmonic mode support by a slot in a thin metal film," Opt. Lett. **30**, 3359-3361 (2005).
3. L. Liu, Z. Han, S. He, "Novel surface plasmon waveguide for high integration," Opt. Express **13**, 6645-6650 (2005).
4. D. F. P. Pile, D. K. Gramotnev, "Channel plasmon-polariton in a triangular groove on a metal surface", Opt. Lett. **29**, 1069-1071 (2004).
5. D. K. Gramotnev, D. F. P. Pile. "Single-mode sub-wavelength waveguide with channel plasmon-polaritons in triangular grooves on a metal surface", Appl. Phys. Lett. **85**, 6323-6325 (2004).
6. S. I. Bozhevolnyi, V. S. Volkov, E. Devaux, T. W. Ebbesen, "Channel plasmon-polariton guiding by subwavelength metal grooves", Phys. Rev. Lett. **95,** 046802 (2005).
7. S. I. Bozhevolnyi, V. S. Volkov, E. Devaux, J.-Y. Laluet, T. W. Ebbesen, "Channel plasmon sub-wavelength waveguide components including interferometers and ring resonators," Nature **440**, 508-511 (2006).
8. D. F. P. Pile, D. K. Gramotnev, M. Haraguchi, T. Okamoto, M. Fukui, "Numerical analysis of coupled wedge plasmons in a structure of two metal wedges separated by a gap," J. Appl. Phys. **100**, 013101 (2006).
9. P. Berini, "Plasmon-polariton waves guided by thin lossy metal films of finite width: Bound modes of symmetric structures," Phys. Rev. B **61**, 10484 (2000).
10. D. F. P. Pile, T. Ogawa, D. K. Gramotnev, T. Okamoto, M. Haraguchi, M. Fukui, S. Matsuo "Theoretical and experimental investigation of strongly localized plasmons on triangular metal wedges for subwavelength waveguiding," Appl. Phys. Lett. **87**, 061106 (2005).
11. Y. Satuby, M. Orenstein, "Surface-Plasmon-Polariton modes in deep metallic trenches- measurement and analysis," Opt. Express **15**, 4247-4252 (2007).
12. D. F. P. Pile, "Compact-2D FDTD for waveguides including materials with negative dielectric permittivity, magnetic permittivity and refractive index," Appl. Phys. B **81**, 607-613 (2005).
13. Y. Satuby, M. Orenstein, "Surface plasmon poloariton waveguiding: From multimode stripe to a slot geometry," Appl. Phys. Lett. **90**, 251104 (2007).

#85683 - $15.00 USD Received 25 Jul 2007; revised 4 Sep 2007; accepted 4 Sep 2007; published 4 Oct 2007

The use of plasmons in guiding metallic structures is one of the most promising approaches for overcoming the diffraction limit of light and significantly increasing levels of integration and miniaturization of integrated optical devices and components. Recently a new type of efficient sub-wavelength waveguide in the form of a narrow gap in a thin metal film (Fig. 1(a)) was independently proposed and analyzed by three groups [1-3] and the corresponding guided plasmon modes experimentally observed [1]. These plasmons can offer several attractive features including broadband guiding with subwavelength localization in two-dimensions, high transmission through sharp bends (due to inefficient leakage through the surrounding metal), high tolerance to structural imperfections, single-mode operation and relatively simple fabrication compared to other plasmon waveguides that offer similar important features (e.g., channel plasmon-polaritons in V-grooves [4-7]).

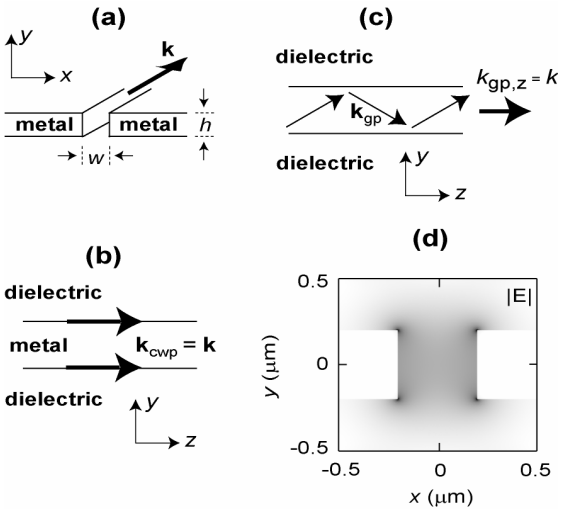

Fig. 1. (a) Gap plasmon waveguide in the form of a rectangular gap (trench) of width, *w*, in a metal film of thickness *h*. (b) Representation of the guided plasmonic modes formed by coupled wedge plasmons at the four corners of the gap. (c) Geometrical optics representation of the higher order modes formed by gap plasmon modes guided by the effective index core formed by the finite thickness of the film. (d) A typical plasmonic mode field (distribution of |*E*|) formed by four coupled wedge plasmons with symmetric (across the thickness of the film) and anti-symmetric (across the gap) distribution of charges; $w = h = 400$ nm, vacuum wavelength $\lambda_{vac} = 1.55$ μm, the gap is made in a gold film ($\varepsilon_{Au} = -96.90 + i10.97$), the dielectric permittivity inside and outside the gap is $\varepsilon_d = 2.25$.

It was shown that a gap in a metal film with a uniform dielectric filling the gap and surrounding regions (Fig. 1(a)) can support two types of mode which are physically distinct in nature [1]. One of these mode types is related to coupled wedge plasmons [1,2,8] that are similar to those formed at the corners of a metallic strip [9] or at the tip of a metal wedge [10]. The wave numbers of these guided plasmonic modes are equal to the wave numbers of the wedge plasmons propagating along the four corners of the gap and coupled across the gap and film (Figs. 1(b,d)). These modes correspond to the four possible coupling symmetries (symmetric and antisymmetric) across the gap and film. The second type of mode is related to a gap plasmon guided by the gap's finite extent along the *y*-axis. If the gap extension along the *y*-axis is finite (Figs. 1(a,c)), then a guided plasmonic mode is formed as a result of successive reflections of the gap plasmon from the top and the bottom of the guiding trench, similar to how a bulk wave is guided by a slab to form a guided slab mode (Fig. 1(c), see also [1,3]) . Both types of mode have been considered in the literature for various wavelengths, gap widths and thicknesses of the film between identical [1,3] and different dielectric media [2,3].

#85683 - $15.00 USD Received 25 Jul 2007; revised 4 Sep 2007; accepted 4 Sep 2007; published 4 Oct 2007

The recent paper by Satuby and Orenstein [11] claims the existence of long-range surface plasmon-polariton eigenmodes in the structure with a wide (several microns) gap in a metal film surrounded by a uniform dielectric medium. However, in our opinion, the results obtained in [11] are not consistent with guided long-range plasmonic modes. Therefore, the aim of this paper is to present a detailed numerical analysis of the structures considered in [11], determine and analyze plasmonic structural eigenmodes, and demonstrate that the long-range plasmonic modes in question do not exist. We also show that the experimental results obtained in [11] are consistent with beams of bulk waves and non-localized (to the gap) surface plasmons propagating (and diffracting) in the considered structures.

For our numerical analysis we use the same structural parameters as in [11]: 400 nm thick gold films ($\varepsilon_{Au} = -96.90 + i10.97$); vacuum wavelength $\lambda_{vac} = 1.55$ μm; and the gold film (and the gap) is surrounded by (filled with) a uniform dielectric with the permittivity $\varepsilon_d = 2.25$. The numerical results presented here are from the commercial finite-element frequency-domain solver of Maxwell's equations (COMSOL). These results have also been verified by two previously developed and tested in-house numerical algorithms: a 3D finite-difference time-domain (FDTD) solver [1,10,12], and a compact-2D FDTD mode-solver [1,8,10,12].

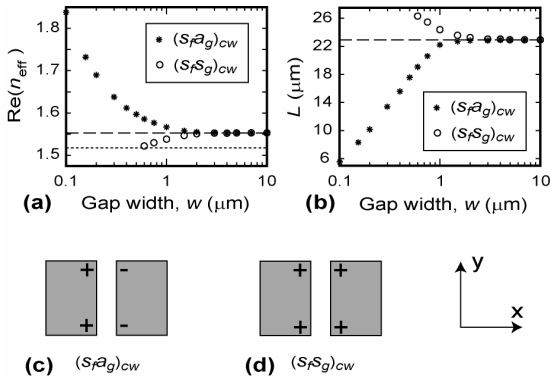

Fig. 2. (a) The dependencies of the real parts of the effective mode indices $\mathrm{Re}(n_{eff}) = \mathrm{Re}[k\lambda_{vac}/(2\pi)]$ and (b) propagation distances $L = 0.5/\mathrm{Im}(k)$ on the gap width w for the $(s_f a_g)_{cw}$ (asterisks) and $(s_f s_g)_{cw}$ (circles) plasmonic modes. The dashed straight lines correspond to the effective index (a) and propagation distance (b) for the $(s_f a_g)_{cw}$ and $(s_f s_g)_{cw}$ modes at the infinite gap width. The dotted straight line corresponds to the effective index for surface plasmons at the top and bottom interfaces of the gold film. (c,d) Representation of the charge distribution for (c) the $(s_f a_g)_{cw}$ mode (with the charge distribution symmetric across the film and antisymmetric across the gap), and (d) the $(s_f s_g)_{cw}$ mode (with the charge distribution symmetric across the film and gap). $w = 400$ nm, $\lambda_{vac} = 1.55$ μm, permittivity of the dielectric inside and outside the gap $\varepsilon_d = 2.25$, and $\varepsilon_{Au} = -96.90 + i10.97$.

Figure 2(a) shows the real parts of the effective refractive indices $\mathrm{Re}(n_{eff}) \equiv \mathrm{Re}[k\lambda_{vac}/(2\pi)]$ for the two existing plasmonic eigenmodes in the considered structure as functions of the gap width w. Here, k is the wave number of the guided plasmonic mode in the gap. The fundamental mode is formed by the coupled wedge plasmons whose electric field distribution [1] corresponds to the charge distribution that is symmetric across the film and antisymmetric across the gap (Fig. 2(c)). We will use the symbol $(s_f a_g)_{cw}$ to denote this fundamental plasmonic mode to reflect the corresponding symmetry of the charge distribution across the film (index f) and across the gap (index g); the indices cw indicate that this mode is formed by coupled wedge plasmons. If the gap width is smaller than the penetration depth of the plasmon field, the symmetry of the fundamental plasmonic mode ($(s_f a_g)_{cw}$) results in a strong attractive interaction of the opposite electric charges across the gap, leading to the strongest mode localization and largest (compared to any other mode in the considered structure) effective refractive index (i.e. the smallest phase velocity) [1]. In this case, the effective

#85683 - $15.00 USD Received 25 Jul 2007; revised 4 Sep 2007; accepted 4 Sep 2007; published 4 Oct 2007

refractive index n_{eff} (and mode localization) increases with decreasing gap width and/or film thickness (Fig. 2(a) and see also [1]). Therefore, the $(s_f a_g)_{cw}$ mode does not have a minimum cut-off film thickness or gap width. This mode was also considered in [2].

As can be seen from Fig. 2(a), the plasmonic $(s_f s_g)_{cw}$ eigenmodes with the $s_f s_g$ symmetry of the charge distribution (Fig. 2(d)) can only exist at gap widths $w \geq 0.6$ μm. If w is reduced below 0.6 μm, the repulsive interaction between the same charges across the gap makes n_{eff} for the $(s_f s_g)_{cw}$ mode smaller than that for the surface plasmons on the top and bottom interfaces of the gold film (dotted line in Fig. 2(a)). The $(s_f s_g)_{cw}$ mode becomes non-eigen, i.e., leaking into the non-localized surface plasmons. Increasing the gap width results in reducing the repulsive interaction of charges across the gap, thus increasing the effective refractive index for the $(s_f s_g)_{cw}$ mode (Fig. 2(a)). If the gap width is significantly larger than the penetration depth of the electromagnetic field into the dielectric, the effect of symmetry of the charge distribution across the gap becomes negligible (see the field distribution for the $(s_f a_g)_{cw}$ mode in Fig. 3(a) for the gap width w = 6 μm which is the smallest gap width considered in [11]). Therefore, at large gap widths the effective mode indices of both the $(s_f a_g)_{cw}$ and $(s_f s_g)_{cw}$ modes tend to the same value (Fig. 2(a)). Physically, this value is equal to the effective index for the plasmon mode guided by the two 90° coupled wedges formed by a rectangular cross-section of the metal film, i.e., when the gap width is equal to infinity (Fig. 3(b)). The effective mode index in this case is $n_{eff} \approx 1.553 + i0.0054$, the real part of which is given by the dashed line in Fig. 2(a).

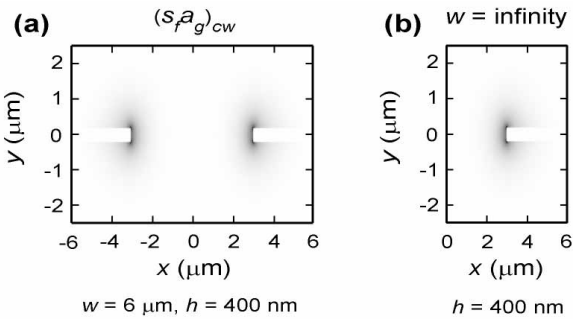

Fig. 3. The distributions of the magnitude of the electric field $|E|$ in (a) the $(s_f a_g)_{cw}$ mode at large gap width w = 6 μm in a gold film ($\varepsilon_{Au} = -96.90 + i10.97$, λ_{vac} = 1.55 μm) of 400 nm thickness imbedded in the uniform dielectric medium with the permittivity ε_d = 2.25, and (b) the plasmon mode guided by the two 90° coupled wedges formed by a rectangular cross-section of the gold film (i.e., at $w = \infty$). Note that the distributions of |E| and |H| are similar for these eignemodes, e.g. having maxima at the same locations, etc.

Note that at large gap widths (e.g., at w = 6 μm in Fig. 3(a)), the differences between the distributions of electric field magnitude in the $(s_f a_g)_{cw}$ and $(s_f s_g)_{cw}$ modes are negligible, and Fig. 3(a) may equally be used to represent either of these modes. Increasing the gap width only results in further separation of the wedge plasmons coupled across the gap, and further reduction of the field in the middle of the gap.

Typical propagation distances for the two $(s_f a_g)_{cw}$ and $(s_f s_g)_{cw}$ modes in the considered structure are presented in Fig. 2(b) as functions of gap width. As can be seen from Fig. 2(b), the maximal propagation distance corresponds to the $(s_f s_g)_{cw}$ mode and is ≈ 26 μm. Clearly, this is not a long-range mode. For comparison, the propagation distance for a non-localized surface plasmon on a smooth gold-dielectric interface (corresponding to λ_{vac} = 1.55, $\varepsilon_{Au} = -96.90 + i10.97$, and ε_d = 2.25) is ≈ 61 μm.

The numerical analysis also suggests that no other plasmonic eigenmodes (including those of the second type) exist at the gap widths and film thicknesses considered in [11]. Indeed, Fig. 4(a) shows the dependencies of the real parts of the effective refractive indices

#85683 - $15.00 USD Received 25 Jul 2007; revised 4 Sep 2007; accepted 4 Sep 2007; published 4 Oct 2007

for the $(a_f a_g)_{cw}$ (circles), $(s_f a_g)_{gp1}$ (crosses), and $(a_f a_g)_{gp1}$ (squares) plasmonic modes. The indices *gp* for the last two modes indicate that these modes are formed by gap plasmons (Fig. 1(c)) rather than coupled wedge plasmons (Figs. 1(b,d)); the additional index 1 is used to denote the order of these modes, because higher order *gp*-type plasmonic modes (e.g., the $(s_f a_g)_{gp2}$ mode) can in principle exist in the considered gap plasmon waveguides (but at significantly smaller gap widths). Note also that the *gp*-modes always correspond to anti-symmetric charge distribution across the gap. (Symmetric *gp*-plasmons always leak into surface plasmons because the repulsive interaction of the same charges across the gap always results in reducing their wave vector below that of surface plasmons.) Nevertheless, to preserve the consistency of notation, we will formally include the symbol a_g in brackets when denoting these modes.

Figure 4(a) demonstrates that the existence of the $(a_f a_g)_{cw}$, $(s_f a_g)_{gp1}$, and $(a_f a_g)_{gp1}$ plasmonic modes in the considered structures is limited to very small gap widths. For example, the respective upper cut-off gap widths for these modes are ≈ 36 nm, ≈ 8.7 nm and ≈ 4.5 nm (Fig. 3(a)). These upper cut-off widths are considerably smaller than the gap widths of 6 – 12 μm considered in [11]. In particular, it follows from here that, contrary to the suggestion made in the third paragraph of section 2 in paper [11], that the walls of the gap can not support single SPPs or coupled *gp*-modes at gap widths of 6 – 12 μm. Therefore, the coupled plasmons propagating on the sides of the gap (trench) cannot be the source for the main field lobe of the trench mode, as was incorrectly (in our opinion) suggested in the third paragraph of section 2 in paper [11].

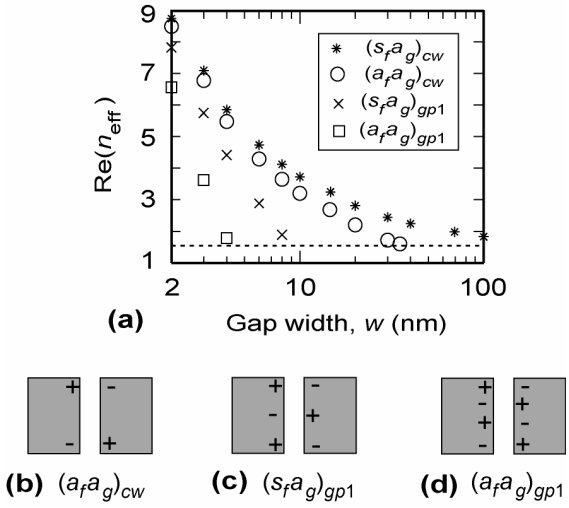

Fig. 4. (a) The dependencies of the real part of the effective mode index n_{eff} on gap width w for the $(s_f a_g)_{cw}$ (asterisks), $(a_f a_g)_{cw}$ (circles), $(s_f a_g)_{gp1}$ (crosses), and $(a_f a_g)_{gp1}$ (squares) plasmonic modes. The dotted straight line corresponds to the effective index for the surface plasmon at the top and bottom interfaces of the gold film. (b-d) Charge symmetries in the gap, corresponding to the (b) $(a_f a_g)_{cw}$, (c) $(s_f a_g)_{gp1}$, and (d) $(a_f a_g)_{gp1}$ plasmonic modes. The other structural parameters are the same as for the previous Figs.

Moreover, as can be seen from Figs. 2(a-c) and 3(a-c) from [11], the field structure in the gap (trench) demonstrates a clear maximum in the middle of the gap. However, if this field were largely due to the coupling of two surface plasmons on either side of the trench (as suggested in the third paragraph of section 2 in [11]), then the field maximums would be at the sides of the gap, but not in the middle of it, because the plasmon field should exponentially decay away from the gold surface (i.e., into the gap). (Note that the E and H fields have similar field distribution, e.g. exhibiting maxima at the same locations, etc.) The penetration depth of the surface plasmon into the dielectric at the considered wavelength (1.55

#85683 - $15.00 USD Received 25 Jul 2007; revised 4 Sep 2007; accepted 4 Sep 2007; published 4 Oct 2007

μm) is ~ 1 μm. Because the width of the trench considered in [11] was 6 – 10 μm, any plasmons on the opposite sides of the trench can hardly be coupled, and the field due to eigenmodes (if they exist) in the trench must be approximately zero, except for the regions of ~ 1 μm thickness near the sides of the trench (which is also demonstrated by Fig. 3(a) – see above). This is in sharp contradiction with the experimental results demonstrated by Figs. 2(a-c) and 3(a-c) from paper [11].

Furthermore, the effective refractive indices for the suggested "long-range plasmonic modes" were found to be $n_{eff} = 1.496 + 0.000164i$ (for the trench of 6 μm width) and $n_{eff} = 1.49768 + 0.0000513i$ (for the trench of 10 μm width) [11]. The real parts of these effective indices are both smaller than the refractive index of the surrounding dielectric ($n_d = 1.50$) and effective refractive index for surface plasmons at the top and bottom interfaces of the metal film ($n_{SP} = 1.518$). This means that the suggested "long-range plasmonic modes" cannot be structural eigenmodes, because such modes would be leaking into both the surrounding dielectric medium and surface plasmons at the film interfaces.

Unfortunately, it is difficult to judge the reasons for the experimental results for TE polarization presented in Figs. 4(a-d) of [11], because the (numerical and experimental) field distributions are identical (probably by mistake) to Figs. 3(a-d) of [11] that show field distributions for the TM polarization [11].

As a result, in our opinion, the experimental results and field distributions obtained in [11] are not consistent with localized plasmonic modes, but are rather the result of propagation of a bulk electromagnetic beam (of ~ 6 – 10 μm in diameter) and non-localized surface plasmons at the gold film interfaces, resulting from the end-fire excitation in the trench. Diffractional divergence of the bulk beam and its partial dissipation in the nearby metal (forming the gap) naturally result in its decaying amplitude along the direction of propagation, giving the illusion of a "long-range" weakly dissipating plasmonic mode. Because dissipative and diffraction effects are stronger near the edges of the beam (i.e., near the sides of the gap), the field distribution has a natural maximum in the middle of the gap (see Figs. 2(a-c) and 3(a-c) from [11]).

The existence of long-range plasmonic modes, discovered by Berini [9] in a thin metal strip surrounded by a uniform dielectric, is related to the film plasmon with anti-symmetric charge distribution across the thickness of the metal strip. Due to this particular charge distribution, the long-range strip plasmon has the wave vector that is smaller than the wave vector of the surface plasmon at the smooth metal-dielectric interface, which ensures its large penetration depths into the surrounding dielectric media and thus weak dissipation in the metal strip. A similar situation is not possible for the inversed structure, where the metal strip is replaced by the gap (trench) in the metal film. Indeed, any plasmon in the gap that has the wave vector that is smaller than that of the surface plasmons at the film interfaces (which is essential for achieving weak dissipation and long-range propagation) will inevitably leak into these surface plasmons at some angle away from the gap (according to the momentum matching), and thus will not be a structural eigenmode.

In conclusion, in our opinion, the suggestion of paper [11] about the discovery of new "long-range plasmonic modes" does not seem to be supported by the experimental results and numerical modeling, and thus is likely to be incorrect. The observed field distributions [11] may naturally be explained by propagation of beams of bulk electromagnetic radiation and generation of surface plasmons at the top and bottom interfaces of the metal film, which has nothing to do with localized plasmonic modes. These conclusions are also supported by the detailed analysis of the two different types of plasmonic eigenmodes in the considered structure conducted in the current paper. Physical interpretation of these modes, their field distributions and propagation distances have been presented, demonstrating agreement between the numerical results and physical expectations. None of the described modes appear to be a long-range plasmonic mode. It should be noted that a related paper was recently published [13] that considered the similar structure as [11] but with thin films and in our opinion also contains significant errors.

#85683 - $15.00 USD Received 25 Jul 2007; revised 4 Sep 2007; accepted 4 Sep 2007; published 4 Oct 2007